



Self-Generation of Surface Roughness by Low-Surface-Energy Alkyl Chains for Highly Stable Superhydrophobic/Superoleophilic MOFs with Multiple Functionalities

Neng-Xiu Zhu[†], Zhang-Wen Wei[†], Cheng-Xia Chen, Dawei Wang, Chen-Chen Cao, Qian-Feng Qiu, Ji-Jun Jiang, Hai-Ping Wang, and Cheng-Yong Su*

Dedicated to Prof. Jean-Marie Lehn on the occasion of his 80th birthday

Abstract: We transformed the hydrophilic metal–organic framework (MOF) **UiO-67** into hydrophobic **UiO-67-Rs** (R = alkyl) by introducing alkyl chains into organic linkers, which not only protected hydrophilic Zr₆O₈ clusters to make the MOF interspace superoleophilic, but also led to a rough crystal surface beneficial for superhydrophobicity. The **UiO-67-Rs** displayed high acid, base, and water stability, and long alkyl chains offered better hydrophobicity. Good hydrophobicity/oleophilicity were also possible with mixed-ligand MOFs containing metal-binding ligands. Thus, a (super)hydrophobic MOF catalyst loaded with Pd centers efficiently catalyzed Sonogashira reactions in water at ambient temperature. Studies of the hydrophobic effects of the coordination interspace and the outer surface suggest a simple *de novo* strategy for the synthesis of superhydrophobic MOFs that combine surface roughness and low surface energy. Such MOFs have potential for environmentally friendly catalysis and water purification.

Introduction

Superhydrophobicity is known for a surface with a water contact angle close to or higher than 150°. The two most important factors contributing to superhydrophobicity are surface roughness and low surface energy.^[1,2] Superhydrophobic materials have long been explored owing to their potential application in anticorrosion, anti-icing, self-cleaning, microfluidic devices, textiles, oil/water separation, water purification, and other applications.^[3–7] Inspired by the natural lotus effect, two main synthetic strategies can be used for the fabrication of a superhydrophobic surface, namely, creating a rough surface or introducing low-surface-energy materials.^[1,2] In the last decade, owing to widespread applications, such as separation,^[9–12] catalysis,^[13] sensing,^[14,15] trans-

porting,^[16] and so on,^[17–19] interest in hydrophobic metal–organic frameworks (MOFs) has burgeoned,^[8] since a critical issue for the real-world use of MOFs is to assess their stability. Surprisingly, of more than 20000 known MOFs,^[20] only a very limited portion exhibit both the thermal and chemical stability desired for harsh environments, especially under water/moisture and acid/base conditions.^[21]

To construct stable waterproof MOFs without the propensity to undergo degradation in the presence of moisture, a common approach is to introduce hydrophobic moieties into the framework or onto the crystal surface, either through *de novo* synthesis^[22–24] or through postsynthetic modification (PSM).^[25,26] This kind of approach mainly focuses on lowering the surface free energy. For example, Omary and co-workers synthesized fluorinated MOFs with superior hydrophobicity for oil-spill cleanup and hydrocarbon storage.^[23] Jiang and co-workers reported a method for coating polydimethylsiloxane (PDMS) on the **UiO-66** crystal to improve its hydrophobicity, catalytic activity, and selectivity.^[27] Recently, the Yamashita group introduced C₇ alkyl chains onto **MIL-125-NH₂** by PSM to enable the photocatalytic production and spontaneous separation of H₂O₂/benzaldehyde in a benzyl alcohol/water two-phase system.^[28] In contrast, the synthetic approach focused on the fabrication of a rough surface, which is popular for carbon- and metal-based hydrophobic materials, remains in its infancy. Kitagawa and co-workers reported an example, in which they synthesized superhydrophobic porous coordination polymers by incorporating an anisotropic crystal morphology with external surface corrugation.^[29]

Herein, we demonstrate the discovery of a one-step bottom-up approach for the construction of superhydrophobic/superoleophilic MOFs with both a rough surface and low surface energy by simply introducing a sufficient amount of alkyl chains (Figure 1). A series of MOFs named **UiO-67-Rs** (R = ethyl, n-butyl, n-hexyl, or n-octyl) with the isostructure of **UiO-67**^[21] were prepared and showed gradually enhanced hydrophobicity as the alkyl chains on the ligand were extended from C₂ to C₈ (Figure 2), as well as excellent chemical stability. Based on a thorough evaluation of the hydrophobicity with regard to the MOF structure, crystal morphology/growth/treatment, and alkyl-chain length/proportion, we developed hydrophobic MOF catalysts **UiO-67-Oct-L²-X%-Pd^{II}** with mixed ligands (Oct stands for a ligand containing a C₈ chain, L² = 2,3'-bipyridine-5,6'-dicarboxylic acid, X% is the L² percentage). In contrast to the hydrophilic **UiO-67-L²-36.4%-Pd^{II}** counterpart and other known MOF

[*] N.-X. Zhu,^[†] Prof. Z.-W. Wei,^[†] Dr. C.-X. Chen, Dr. D.-W. Wang, C.-C. Cao, Q.-F. Qiu, Prof. J.-J. Jiang, Dr. H.-P. Wang, Prof. C.-Y. Su
MOE Laboratory of Bioinorganic and Synthetic Chemistry
Lehn Institute of Functional Materials
School of Chemistry, Sun Yat-Sen University
Guangzhou 510275 (China)
E-mail: cecscy@mail.sysu.edu.cn

[†] These authors contributed equally to this work.

Supporting information and the ORCID identification number(s) for the author(s) of this article can be found under:
<https://doi.org/10.1002/anie.201909912>.

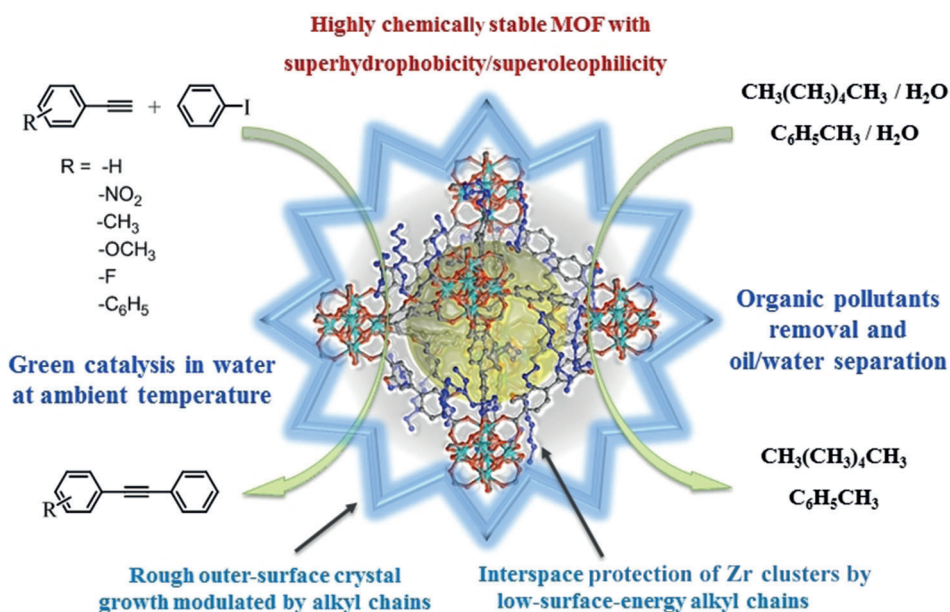


Figure 1. Multifunctional superhydrophobic/superoleophilic MOFs constructed by virtue of simultaneous coordination supramolecular engineering of the interspace and outer surface.

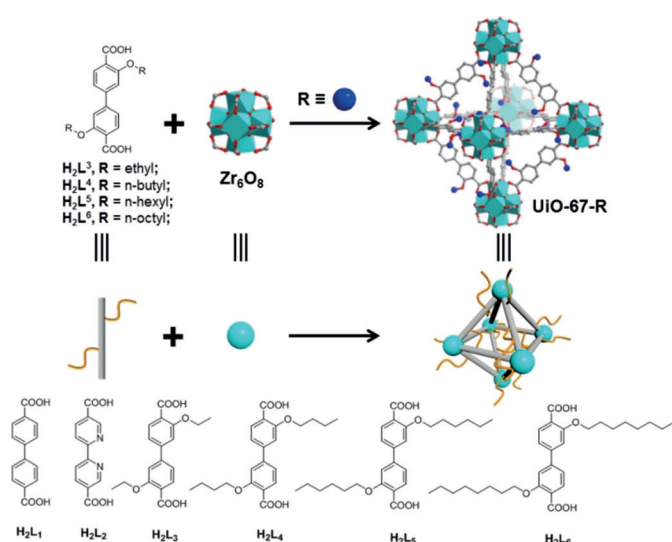


Figure 2. Construction of UiO-67-Rs from Zr₆O₈ clusters and H₂Lⁿ (n = 3–6) linkers containing alkyl chains.

catalysts, the resulting superhydrophobic **UiO-67-Oct-L²-35.7%-Pd^{II}** exhibited remarkably higher catalytic activity and recyclability for Sonogashira reactions in a water medium at a mild temperature. Removal of toluene from water and oil/water separation experiments demonstrated the excellent adsorption and separation capacity resulting from the superoleophilicity of the coordination interspace and the superhydrophobicity of the MOF outer surface. These results point to a facile coordination supramolecular engineering approach to construct superhydrophobic MOFs for multiple purposes without postprocessing of the sample surface or the introduction of extralong hydrophobic moieties.

Results and Discussion

Synthesis, porosity, and stability of UiO-67-Rs

The linear dicarboxylic acid ligands H₂Lⁿ (n = 3, 4, 5, 6) modified with C₂–C₈ alkyl chains were readily prepared starting from methyl 2-hydroxy-4-iodobenzoate (see Scheme S1 and synthetic details in the Supporting Information). The **UiO-67-R** MOFs were synthesized by solvothermal reactions of ZrCl₄ and the corresponding ligands in *N,N*-dimethylformamide (DMF) with trifluoroacetic acid as a modulator at 120 °C for 34 h (Figure 2, see details in the Supporting Information). The powder X-ray diffraction (PXRD) patterns of the **UiO-67-Rs** showed characteristic peaks indexed to **UiO-67**, thus indicating that they are isostructures of **UiO-67** with *fcu* topology (see Figure S1 in the Supporting Information, Zr₆ cluster acting as a 12-c node).^[21] The neat PXRD patterns manifest good crystallinity and phase purity of bulk samples. A simulation of the **UiO-67-R** structures on the basis of an octahedral building unit revealed that the alkyl chains are distributed in the coordination interspace both inwardly and outwardly (see Figure S1), thus suggesting that they can modulate both the interior pore surface and crystal outer surface. The longer alkyl chains are closer to Zr₆O₈ clusters, indicative of better protection of hydrophilic Zr₆O₈ clusters by long alkyl chains. The existence of alkyl-chain-functionalized linkers in **UiO-67-Rs** was also verified by ¹H NMR measurements with the digested crystals (see Figures S2–S5).

To evaluate the porosity of as-prepared **UiO-67** and **UiO-67-Rs**, we conducted N₂ adsorption isotherm measurements at 77 K with activated samples (see Figures S6–S12). All MOFs exhibited type I adsorption isotherms with saturation amounts of 707, 356, 245, 201, and 150 mL g⁻¹ for **UiO-67**, **UiO-67-Et**, **UiO-67-But**, **UiO-67-Hex**, and **UiO-67-Oct**, re-

spectively. The apparent Brunauer–Emmett–Teller (BET) surface area and the total pore volume of **UiO-67-Rs** dropped from 1303 to 349 m^2g^{-1} and from 0.48 to 0.21 mL g^{-1} , respectively, as the length of the alkyl chain increased, and all values were smaller than those of **UiO-67** (2761 m^2g^{-1} , 0.97 mL g^{-1}), whereas the pore sizes (11.7–11.2 Å) calculated by the DFT method remain comparable (see Figure S12 and Table S1 in the Supporting Information). These results are in accordance with the introduction of bulky alkyl chains into the MOF pores with the framework unchanged.

Thermogravimetric analysis (TGA) indicated that all as-prepared MOFs contained a large amount of solvent, which could be evacuated by heating (see Figure S13). Variable-temperature PXRD measurements indicated that **UiO-67-Rs** had thermal stability up to 300 °C, which is lower than that of **UiO-67** owing to the presence of C_8 chains linked by alkoxy oxygen atoms (see Figure S14). To investigate the chemical stability of these MOFs, fresh samples of **UiO-67** and **UiO-67-Rs** were immersed in aqueous solution with different pH values. PXRD revealed that **UiO-67-Et** retained high crystallinity after exposure to a harsh chemical environment in solution at pH 1 and 100 °C for 5 days, whereas **UiO-67-But**, **UiO-67-Hex**, and **UiO-67-Oct** remained stable even longer for at least 20 days. In contrast, **UiO-67** was degraded after only 3 h (see Figure S15). When immersed in solution at pH 12 and 100 °C, **UiO-67-Et** maintained its crystallinity for 3 days, **UiO-67-But** remained unchanged for 11 days, and **UiO-67-Hex** and **UiO-67-Oct** survived for at least 20 days, in contrast to **UiO-67**, which lost crystallinity in only 2 h (see Figure S16). In a solution at pH 13 at room temperature, **UiO-67-Et**, **UiO-67-But**, **UiO-67-Hex**, and **UiO-67-Oct** still survived for 2, 3, 18, and 21 h, respectively (see Figure S17). When treated with fresh water at 100 °C, **UiO-67-Et** retained crystallinity for 5 days, whereas **UiO-67-But**, **UiO-67-Hex**, and **UiO-67-Oct** remained intact for at least 20 days and were thus much more stable than **UiO-67**, which degraded after 10 h (see Figure S18). The good porosity retained after water and acid/base treatment was verified by N_2 adsorption isotherms of the **UiO-67-Oct** sample (see Figure S19). The above results highlight the high chemical stability of **UiO-67-Rs** toward acidic/basic aqueous solutions and their suitability for application under harsh conditions.

Intrinsic MOF Hydrophobicity and Crystal Growth and Analysis

To check the hydrophobicity of **UiO-67-Rs** as related to the MOF structures, we first performed water vapor adsorption at 298 K. The saturation water uptake of **UiO-67** reached 259.3 mL g^{-1} , which is much higher than those of **UiO-67-Rs** (180.5, 174.5, 144.9, and 83.8 mL g^{-1} for **UiO-67-Et**, **UiO-67-But**, **UiO-67-Hex**, and **UiO-67-Oct**, respectively; Figure 3; see also Figures S20–S21), thus indicating a significant decrease in water adsorption capacity with an increase in alkyl-chain length. As an estimation of overall hydrophobic behavior, the starting points for abrupt water uptake were found at relative pressures P/P_0 of 0.21, 0.22, 0.50, 0.65, and 0.70 for **UiO-67**, **UiO-67-Et**, **UiO-67-But**, **UiO-67-Hex**, and **UiO-67-Oct**, respectively; thus, showing a positive correlation

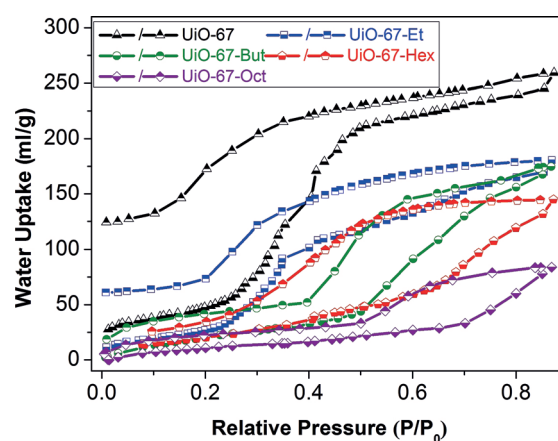


Figure 3. Water adsorption isotherms of **UiO-67** and **UiO-67-Rs** at 298 K.

between increasing hydrophobicity of the MOF pores and the alkyl-chain length. PXRD patterns after water adsorption indicated that the crystallinity of **UiO-67-Rs** remained more intact for the MOFs with longer alkyl chains, in contrast to **UiO-67**, which degrades obviously (see Figure S20). In particular, the water adsorption behavior of **UiO-67-Oct** maintained perfect robustness for three successive cycles (see Figure S21).

Convincing proof for the hydrophobic performance of **UiO-67-Rs** was obtained by measuring the water contact angle (CA), which according to criteria for superhydrophobicity must be no less than 150°. [2] The powder of **UiO-67** is readily wetted by water, indicating a hydrophilic nature (Figure 4; see also Figure S22). For comparison, a water droplet can roll over the **UiO-67-R** powders as over a lotus leaf, thus demonstrating their good hydrophobicity. The CA of a water droplet on **UiO-67-R** powders quickly increases from 121.1 to 154.0° as the alkyl chains are extended from ethyl to n-octyl, clearly confirming that the introduction of alkyl chains on the organic linkers can transform the surface character of **UiO-67** from hydrophilicity to hydrophobicity, and even superhydrophobicity with longer n-hexyl and n-octyl chains. On the other hand, **UiO-67-Oct** is completely wettable with toluene, n-hexane, and dichloromethane, sinking in these organic solvents but floating on water, thus demonstrating its intrinsic superhydrophobicity and superoleophilicity (see Figure S23).

It is reasonable that the alkyl chains are associated with hydrophobicity, favoring a decrease the surface energy of the materials to enhance hydrophobicity. [1] However, CA measurements of the pure H_2L^{3-8} ligands revealed that these organic linkers are actually hydrophilic owing to the carboxylate acid groups (see Figure S24). Hence materials simply containing alkyl chains are not automatically endowed with hydrophobicity, especially as C_2 – C_8 alkyl chains are not as long as those commonly used to coat or modify MOFs for hydrophobicity. [24,27,30,31] As the **UiO-67-Rs** are constructed from essentially hydrophilic Zr_6O_8 clusters and dicarboxylate linkers, we may rationalize that the formation of the porous and ordered framework plays a critical role, whereby the alkyl chains are universally disposed in an appropriate way to

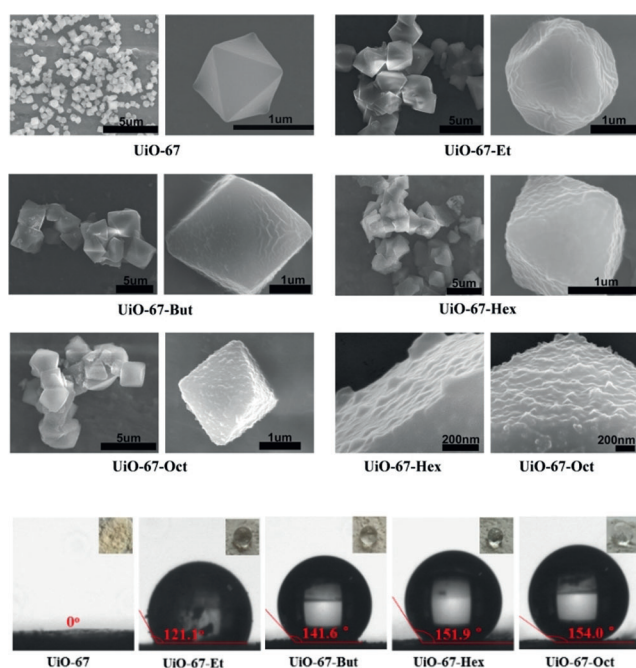


Figure 4. SEM images and digital photographs of static water contact angles of **UiO-67** and **UiO-67-Rs**.

protect the hydrophilic Zr_6O_8 clusters and carboxylate groups, thus providing a hydrophobic effect at the molecular level. To test this hypothesis, we prepared the comparable MOF **UiO-67-*m*-Oct** by introducing C_8 alkyl chains onto the *meta* position of the ligand, not adjacent to the hydrophilic components, which gave a CA value of 132.9° and good wettability with organic solvents (see Figure S25), thus indicating retention of good superoleophilicity but less effective superhydrophobicity. We further damaged **UiO-67-Oct** in basic solutions. The PXRD patterns confirmed that the framework collapsed, with H_2L^6 linkers remaining, as seen by 1H NMR spectroscopy (see Figure S26). Scanning electron microscope (SEM) images showed an amorphous morphology with a water CA of 29.5° . These observations suggest the framework integrity is vital to the hydrophobicity of **UiO-67-Rs**, making the introduced alkyl chains just right for oleophilic pores and a hydrophobic surface.

To get more insight into the hydrophobic effect of **UiO-67-Rs**, we carried out a detailed evaluation of hydrophobicity as correlated with crystal morphology, growth, and treatment. SEM revealed that **UiO-67-Rs** grow into micrometer-sized octahedral crystals, similarly to **proto-UiO-67** (Figure 4). A surprise observation is that, in the presence of alkyl chains, a reentrant texture of the crystal outer surface is generated, like rolling mountains, in contrast to the smooth surface of **UiO-67**. As revealed by Jiang and others,^[2] such micro/nanoscale roughness, like that of a lotus leaf, is a critical factor for water repellence, thus suggesting that the crystal morphology also contributes to the hydrophobic nature of **UiO-67-Rs**. The convex–concave surface is evolved more significantly as the alkyl chains become longer (Figure 4), giving rise to more and more isolating protrusions ranging from dozens to hundreds of nanometers in size. Such increasing tendency

toward surface roughness coincides well with the elongation of the alkyl chains, thus hinting at a stronger ability of longer alkyl chains to self-create a rougher surface. To check if the crystal growth process can affect the hydrophobicity, we prepared a series of **UiO-67-Oct** crystals by controlling the incubation time (Figure 5 a–c; see also Figure S27). It turns

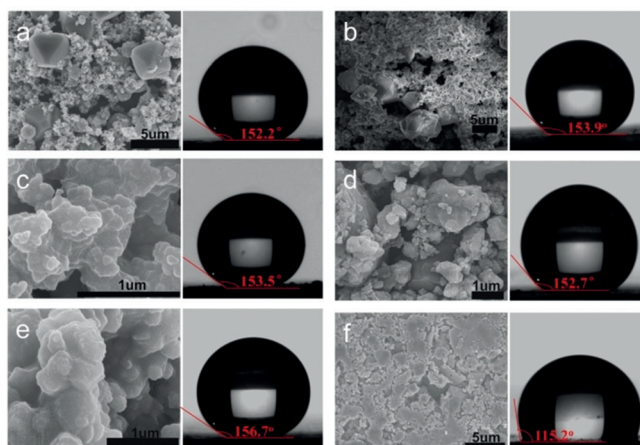


Figure 5. SEM images and static water contact angles of **UiO-67-Oct** crystals obtained with variable incubation times, stirring, grinding, or squeezing: a) **UiO-67-Oct-48 h**, b) **UiO-67-Oct-64 h**, c) **UiO-67-Oct-72 h**, d) **UiO-67-Oct-ground**, e) **UiO-67-Oct-stir**, and f) **UiO-67-Oct-squeezed**.

out that the incubation time has a clear influence on the shape and size of MOF crystals. As the incubation under $120^\circ C$ was extended from 34 to 72 h, the regular octahedral crystals gradually turned into smaller irregular crystalline micro-particles. However, the PXRD patterns verified that the samples kept the isostructural character of **UiO-67** (see Figure S28), and all other properties, such as porosity and thermal, acid/base, and water stability were completely retained (see Figures S29–S38 and Table S2). Most importantly, the water CA was little affected by incubation time, thus indicating that the crystal shape and size had minimal effect on the superhydrophobicity of **UiO-67-Oct**. This finding was supported by a control experiment for which we ground **UiO-67-Oct** crystals. The obtained **UiO-67-Oct-ground** possessed nearly identical properties and superhydrophobicity to **UiO-67-Oct** (Figure 5 d; see also Figures S29–S38). Furthermore, we directly prepared **UiO-67-Oct-stir** by stirring at $120^\circ C$ for 48 h instead of the solvothermal reaction. The product appeared as a crystalline conglomerate with a uniform rough surface and showed similar porosity and thermal stability to that of **UiO-67-Oct**, as well as even better chemical stability and a slightly higher water CA of 156.7° (Figures 5 e; see also Figures S39–S45 and Table S3). This result suggests a facile synthetic route to superhydrophobic **UiO-67-Oct** on a large scale, thus facilitating its practical application.

For comparison, we squeezed **UiO-67-Oct** crystals into sheets with different pressures of 0.2, 0.5, 1.0, and 2.0 t. PXRD patterns indicated that the treated bulky samples still displayed similar crystallinity (see Figure S46); however, SEM images reveal that the surface of the squeezed sheet



becomes more and more smooth as the pressure increases (Figure 5f; see also Figure S47). The water CA of the squeezed sheets decreased continuously from 154.0 to 135.6, 119.4, 115.2, and 100.6° (see Figure S47), showing a clear decrease in the surface hydrophobicity. This result suggests that the flattened surface (decrease in surface roughness) leads to reduction of the surface hydrophobicity, which is likely to be partially caused by destruction of the MOF structure at the surface. We also tried to make a rough surface on hydrophilic **UiO-67** by extending the incubation period or by etching the surface of crystals in methanol with sodium hydroxide. The obtained **UiO-67-34h** and **UiO-67-34h-etching** had PXRD patterns with retained crystallinity (see Figure S48). SEM images showed that **UiO-67-34h** had a slightly rough surface, whereas the surface roughness of **UiO-67-34h-etching** was evident; however, the water CA of **UiO-67-34h** was undetectable, as for **UiO-67**, while that of **UiO-67-34h-etching** was just 10.2° (see Figure S49). This result demonstrates a positive effect of surface roughness toward hydrophobicity; nevertheless, the contribution of low surface energy by alkyl chains is indispensable. Without alkyl chains suitably arranged in a well-ordered framework, hydrophilic **UiO-67** may not be transformed into a hydrophobic MOF merely by fabricating surface roughness.

Hydrophobic Mixed-Ligand MOFs and MOF Catalysts

The superhydrophobicity of **UiO-67-Oct** encouraged us to explore the possibility of constructing hydrophobic mixed-ligand MOFs in order to introduce more functionality. Through changing the molar ratio of H_2L^1 ($\text{H}_2\text{L}^1 = 1,1'$ -biphenyl-4,4'-dicarboxylic acid) to H_2L^6 , a series of **UiO-67-Oct-L¹-X%** MOFs ($X = 37.9, 46.5, \text{ and } 66.7\%$, standing for the L^1 percentage determined by ^1H NMR spectroscopy of digested MOFs) were prepared by solvothermal reactions of H_2L^1 , H_2L^6 , and ZrCl_4 at 120 °C (see Figures S50–S53). Water CA measurements indicated that **UiO-67-Oct-L¹-37.9%** had a high CA value of 150.3°, suggesting superhydrophobic character, whereas those of **UiO-67-Oct-L¹-46.5%** and **UiO-67-Oct-L¹-66.7%** decreased to 140.6 and 121.6°, respectively (Figure 6; see also Figure S54). SEM images confirmed that a rough surface similar to that of **UiO-67-Oct** was successfully achieved for **UiO-67-Oct-L¹-37.9%** (Figure 6). As the percentage of L^6 was reduced, the surface roughness of **UiO-67-Oct-L¹-X%** decreased simultaneously, consistent with a change in hydrophobicity. Therefore, the presence of octyl chains inherently introduces surface roughness, thus contributing to MOF hydrophobicity. The phase purity of bulk samples was confirmed by PXRD patterns (see Figure S55), thermal stability up to 350 °C was testified by TGA analysis (see Figure S56), and significantly, the porosity of the mixed-ligand MOFs was increased to more than twice that of **UiO-67-Oct** (see Figures S57–S61 and Table S4).

Many catalytic reactions take place under harsh conditions, including in water, acid, and alkali media, and demand organic solvents and heating,^[32–35] so the development of green catalysts that operate in water under mild conditions is important and useful. The successful strategy for the synthesis

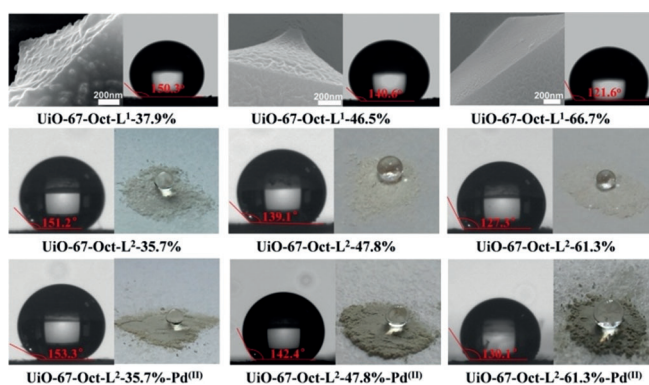


Figure 6. SEM images and static water contact angles of mixed-ligand MOFs **UiO-67-Oct-L¹-X%** and **UiO-67-Oct-L²-X%** and MOF catalysts **UiO-67-Oct-L²-X%-Pd^{II}**.

of the above stable and hydrophobic mixed-ligand **UiO-67-Oct-L¹-X%** MOFs paves the way for the construction of hydrophobic MOF catalysts by replacing L^1 with L^2 , which is then available for metalation to introduce catalytic sites. By combining H_2L^6 with the additional ligand H_2L^2 ($\text{H}_2\text{L}^2 = 2,3'$ -bipyridine-5,6'-dicarboxylic acid) we synthesized a series of precursors **UiO-67-Oct-L²-X%** ($X = 35.7, 47.8, \text{ and } 61.3\%$, standing for the L^2 percentage determined by ^1H NMR spectroscopy of digested MOFs) following the above approach (see Figures S62–S65). Water CA measurements confirmed the superhydrophobicity of **UiO-67-Oct-L²-35.7%** with a CA value of 151.2°, and hydrophobicity of **UiO-67-Oct-L²-61.3%** and **UiO-67-Oct-L²-47.8%** (Figure 6; see also Figure S66). Incubation of **UiO-67-Oct-L²-X%** in acetonitrile with $\text{PdCl}_2(\text{CH}_3\text{CN})_2$ at 65 °C for 24 h successfully led to (super)hydrophobic MOF catalysts **UiO-67-Oct-L²-X%-Pd^{II}** (Figures 6). Inductively coupled plasma atomic emission spectroscopy (ICP-AES) revealed that the Pd loading was 3.38, 5.14, and 7.74 wt% for **UiO-67-Oct-L²-35.7%-Pd^{II}**, **UiO-67-Oct-L²-47.8%-Pd^{II}**, and **UiO-67-Oct-L²-61.3%-Pd^{II}**, respectively (see Table S5), thus indicating nearly quantitative metalation of all H_2L^2 sites. The phase purity, crystal morphology, framework porosity, and thermal stability were verified to be comparable before and after metalation (see Figures S67–S78 and Table S6), and the 2+ oxidation state of the Pd centers was testified by X-ray photoelectron spectroscopy (XPS) analysis (see Figures S83–S90). Moreover, **UiO-67-Oct-L²-35.7%-Pd^{II}** exhibited superhydrophobicity with a CA value of 153.3°, whereas the water CA values of **UiO-67-Oct-L²-47.8%-Pd^{II}** and **UiO-67-Oct-L²-61.3%-Pd^{II}** were 142.4 and 130.1°, respectively (Figure 6). For comparison, we also prepared **UiO-67-L²-36.4%-Pd^{II}** (see Figures S79–S81), which had a CA value of just 22.8° and a hydrophilic nature (see Figure S82).

The typical Sonogashira reaction between aryl halides and phenylacetylene with a Pd catalyst was used to test the effect of hydrophobicity on the heterogeneous catalytic performance of the MOFs (see Figures S91–S105). As a benchmark reaction, iodobenzene and phenylacetylene were first chosen as the substrates to produce diphenylacetylene. Under mild reaction conditions in water at ambient temperature, the reaction catalyzed by superhydrophobic **UiO-67-Oct-L²-**

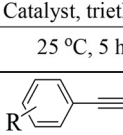
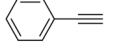
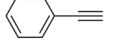
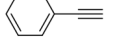
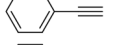
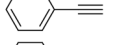
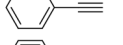
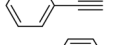
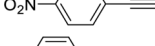
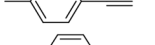
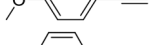
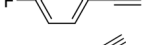
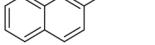
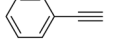
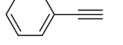
35.7%-Pd^{II} was complete in 5 h to give the product in 91 % yield (Table 1, entry 7), whereas the catalytic yields of hydrophobic **UiO-67-Oct-L²-47.8%-Pd^{II}** and **UiO-67-Oct-L²-61.3%-Pd^{II}** were 85 and 77%, respectively, comparable to or still higher than that of the homogeneous PdCl₂(CH₃CN)₂ catalyst (Table 1, entries 3, 5, and 6). In contrast, hydrophilic **UiO-67-L²-36.4%-Pd^{II}** only offered a low yield of 44% (Table 1, entry 4). These results clearly suggest that higher hydrophobicity of the MOF catalysts leads to higher catalytic efficiency. When the reaction was performed under the same conditions without a catalyst or using **UiO-67-Oct-L²-35.7%** without loaded Pd centers, no product was detected (Table 1, entries 1 and 2), thus confirming that the Pd centers in the MOF catalyze the reaction. To test the scope of the use of **UiO-67-Oct-L²-35.7%-Pd^{II}** for the Sonogashira reaction, we examined various alkynes with different substituents under similar reaction conditions (Table 1, entries 8–12; see also Table S7). Satisfactory conversion was observed for all substrates, whereby 4-nitroethynylbenzene with a strongly electron withdrawing NO₂ group gave the best yield, and others exhibited good conversion in the order CH₃ < CH₃O < F. Notably, a moderate yield of 83% was also observed for the

conversion of 2-ethynyl-naphthalene, thus suggesting that **UiO-67-Oct-L²-35.7%-Pd^{II}** can efficiently catalyze the reaction of bulky substrates.

A hot filtration test was performed to examine the heterogeneous nature of **UiO-67-Oct-L²-35.7%-Pd^{II}**. When the MOF catalyst was removed from the reaction solution after 4 h, no further conversion was observed (see Figure S92). Examination of the Pd and Zr content in the filtrate by ICP indicated neglectable leaching of metal atoms (see Table S8). To check the recyclability and reusability of the MOF catalyst, 10 reaction cycles were performed without changing the **UiO-67-Oct-L²-35.7%-Pd^{II}** catalyst. The reaction yield only dropped a little, thus manifesting strong robustness of the superhydrophobic MOF catalyst (see Figure S93). Monitoring of the **UiO-67-Oct-L²-35.7%-Pd^{II}** catalyst by PXRD for 10 cycles showed that the MOF catalyst retained excellent crystallinity (see Figure S95), and SEM revealed that the MOF catalyst maintained intact octahedral morphology (see Figure S98). In striking contrast, hydrophilic **UiO-67-L²-36.4%-Pd^{II}** lost its catalytic activity quickly in just two cycles (see Figure S94), and PXRD and SEM analysis indicated that its framework collapsed with the formation of

irregular particles after only the second catalytic cycle (see Figures S97 and S98). These results unambiguously suggest that superhydrophobic **UiO-67-Oct-L²-35.7%-Pd^{II}** is competent for efficient and green heterogeneous catalysis; its hydrophobicity can facilitate water-resistant reactions, while its oleophilicity favors the transportation of organic substrates in water. More evidence is provided by control experiments utilizing various organic solvents, in which only low conversion was observed (see Table S9). In contrast to previously reported heterogeneous catalysts for the Sonogashira reaction (see Table S10),^[36–47] superhydrophobic **UiO-67-Oct-L²-35.7%-Pd^{II}** is also able to effectively catalyze the reaction at ambient temperature without heating, thus acting as an environmentally friendly and cost-saving heterogeneous catalyst.

Table 1: Sonogashira reactions under different conditions.^[a]

Entry	Catalyst		Solvent	Yield [%] ^[b]	TOF [h ⁻¹]
1	no catalyst		H ₂ O	0	0
2	UiO-67-Oct-L²-35.7%		H ₂ O	0	0
3	Pd(CH ₃ CN) ₂ Cl ₂		H ₂ O	79	16
4	UiO-67-L²-36.4%-Pd^{II}		H ₂ O	44	9
5	UiO-67-Oct-L²-61.3%-Pd^{II}		H ₂ O	77	15
6	UiO-67-Oct-L²-47.8%-Pd^{II}		H ₂ O	85	17
7	UiO-67-Oct-L²-35.7%-Pd^{II}		H ₂ O	91	18
8	UiO-67-Oct-L²-35.7%-Pd^{II}		H ₂ O	94 ^[c]	19
9	UiO-67-Oct-L²-35.7%-Pd^{II}		H ₂ O	85	17
10	UiO-67-Oct-L²-35.7%-Pd^{II}		H ₂ O	87	18
11	UiO-67-Oct-L²-35.7%-Pd^{II}		H ₂ O	90	18
12	UiO-67-Oct-L²-35.7%-Pd^{II}		H ₂ O	83 ^[c]	17
13	UiO-67-Oct-L²-35.7%-Pd^{II}		DMF	2	0
14	UiO-67-Oct-L²-35.7%-Pd^{II}		CH ₃ CN	8	2

[a] Reaction conditions: catalyst (1.0 mmol% Pd), phenylacetylene (0.5 mmol), iodobenzene (1.0 mmol), triethylamine (1.0 mmol), nitrogen atmosphere, 25 °C, 5 h. [b] Determined by GC–MS.

[c] Determined by ¹H NMR spectroscopy. TOF = turnover frequency.

Removal of Water Pollutants and Oil/Water Separation

To further take advantage of the surface hydrophobicity and channel oleophilicity of **UiO-67-Rs**, we tested the absorption of toluene from water to imitate water purification. After **UiO-67**, **UiO-67-Oct**, or **UiO-67-Oct-L¹-37.9%** (10 mg) was dis-

persed in a toluene-saturated solution (30 mL) for 12 h, UV/Vis spectra revealed that about 68.61, 83.67, and 97.02%, respectively, of the toluene was adsorbed into the MOF pores (Figure 7; see also Figure S106). This observation suggests that the hydrophobic MOFs can remove toluene from water more efficiently than hydrophilic MOFs, and the mixed-ligand **UiO-67-Oct-L¹-37.9%** with larger pores is more effective than **UiO-67-Oct** with comparable hydrophobicity.

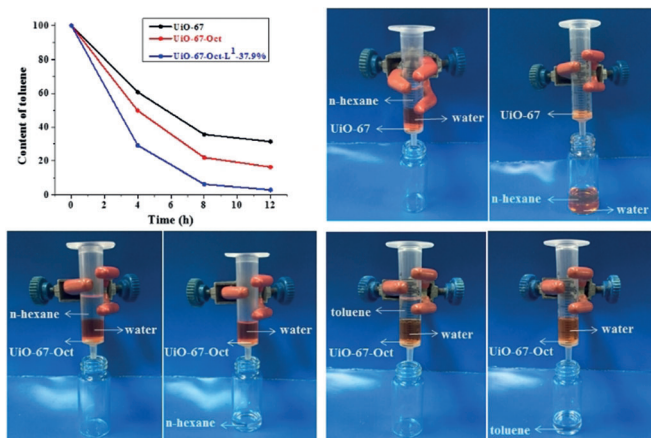


Figure 7. UV/Vis spectral absorbance decrease showing toluene removal from water by **UiO-67**, **UiO-67-Oct**, and **UiO-67-Oct-L¹-37.9%**, and digital photographs of oil/water separations by **UiO-67** and **UiO-67-Oct**. The water was dyed with methyl orange for clear observation.

As a chemically stable bifunctional MOF, superhydrophobic and superoleophilic **UiO-67-Oct** was expected to have potential for application in oil/water separation. The separation equipment was homemade and fabricated according to a previously reported method.^[31,48] After assembling the filter device with **UiO-67-Oct**, n-hexane/water and toluene/water separation were tested. The separation process is shown in Figure 7 (see also videos in the Supporting Information), as well as the oil/water mixture before and after filtration through the **UiO-67-Oct** samples. When a mixture of water (dyed with methyl orange) and n-hexane (or toluene) was gravity fed into the syringe tube, two layers formed. Moving of a plastic straw back and forth to mix the oil with the water enabled n-hexane (or toluene) to pass freely through the **UiO-67-Oct** sheet and fall into the vial underneath, but water could not penetrate the superhydrophobic filter. A similar test was conducted with a **UiO-67** separation setup; in this case, both phases could pass through the **UiO-67** filter. These results verify that superhydrophobic **UiO-67-Oct** has an efficient oil/water separation ability, but hydrophilic **UiO-67** is ineffective.

Conclusion

In summary, a series of hydrophobic MOFs have been successfully synthesized through a simple coordination supramolecular engineering strategy by introducing C₂–C₈ alkyl chains onto the organic linkers of **UiO-67**, thus providing

UiO-67-Rs with a high level of chemical stability towards acid/basic aqueous solutions in comparison with hydrophilic **proto-UiO-67** and known hydrophobic MOFs (see Table S11). The framework enables the appropriate arrangement of alkyl chains in the coordination interspace to protect hydrophilic Zr₆O₈ clusters and carboxylate groups, thus leading to hydrophobicity of a chemical nature at the molecular level. The introduction of alkyl chains simultaneously enables the self-generation of a rough crystal surface. In this way, the combination of two important factors, surface roughness and low surface energy, in crystal growth leads to superhydrophobicity. Moreover, the presence of alkyl chains in the framework pores also makes the superhydrophobic MOFs superoleophilic, which facilitates the absorption of lipophilic organic compounds and water pollutants, as well as oil/water separation. The success of this facile synthetic approach has further been extended to the preparation of mixed-ligand superhydrophobic MOFs, thus offering an opportunity to introduce more functionality. In this way, the (super)hydrophobic MOF catalyst **UiO-67-Oct-L²-35.7%-Pd^{II}** was constructed. This green heterogeneous catalyst exhibited excellent catalytic activity, recyclability, and reusability under aqueous and mild conditions. It is envisioned that this straightforward strategy without post-coating or rough-surface fabrication processes may open a new avenue for the design of multifunctional superhydrophobic MOF materials for practical application in an economical and environmentally friendly fashion.

Acknowledgements

We are grateful for financial support by the NSFC (21603278, 21821003, 21720102007, 21573291, 21890380), the LIRT Project of GPRTP (2017BT01C161), Chinese Postdoctoral Science Fund (2017M622866), the International Postdoctoral Exchange Fellowship Program (20180055), and the FRF for the Central Universities.

Conflict of interest

The authors declare no conflict of interest.

Keywords: green chemistry · metal–organic frameworks · superhydrophobicity · superoleophilicity · water purification

- [1] X. Zhang, F. Shi, J. Niu, Y. Jiang, Z. Wang, *J. Mater. Chem.* **2008**, *18*, 621–633.
- [2] L. Feng, S. Li, Y. Li, H. Li, L. Zhang, J. Zhai, Y. Song, B. Liu, L. Jiang, D. Zhu, *Adv. Mater.* **2002**, *14*, 1857–1860.
- [3] B. N. Sahoo, B. Kandasubramanian, *RSC Adv.* **2014**, *4*, 22053–22093.
- [4] Q. Sun, H. He, W.-Y. Gao, B. Aguila, L. Wojtas, Z. Dai, J. Li, Y.-S. Chen, F.-S. Xiao, S. Ma, *Nat. Commun.* **2016**, *7*, 13300.

- [5] T. Darmanin, F. Guittard, *J. Mater. Chem. A* **2014**, *2*, 16319–16359.
- [6] Q. Sun, B. Aguila, G. Verma, X. Liu, Z. Dai, F. Deng, X. Meng, F.-S. Xiao, S. Ma, *Chem* **2016**, *1*, 628–639.
- [7] Q. Sun, B. Aguila, J. A. Perman, T. Butts, F.-S. Xiao, S. Ma, *Chem* **2018**, *4*, 1726–1739.
- [8] R. Antwi-Baah, H. Liu, *Materials* **2018**, *11*, 2250–2270.
- [9] C.-X. Chen, Z.-W. Wei, J.-J. Jiang, S.-P. Zheng, H.-P. Wang, Q.-F. Qiu, C.-C. Cao, D. Fenske, C.-Y. Su, *J. Am. Chem. Soc.* **2017**, *139*, 6034–6037.
- [10] J. B. DeCoste, G. W. Peterson, *Chem. Rev.* **2014**, *114*, 5695–5727.
- [11] Y. He, W. Zhou, G. Qian, B. Chen, *Chem. Soc. Rev.* **2014**, *43*, 5657–5678.
- [12] R. Zou, A. I. Abdel-Fattah, H. Xu, Y. Zhao, D. D. Hickmott, *CrystEngComm* **2010**, *12*, 1337–1353.
- [13] J. Liu, L. Chen, H. Cui, J. Zhang, L. Zhang, C.-Y. Su, *Chem. Soc. Rev.* **2014**, *43*, 6011–6061.
- [14] Z. Hu, B. J. Deibert, J. Li, *Chem. Soc. Rev.* **2014**, *43*, 5815–5840.
- [15] L. Chen, J.-W. Ye, H.-P. Wang, M. Pan, S.-Y. Yin, Z.-W. Wei, L.-Y. Zhang, K. Wu, Y.-N. Fan, C.-Y. Su, *Nat. Commun.* **2017**, *8*, 15985.
- [16] M.-X. Wu, Y.-W. Yang, *Adv. Mater.* **2017**, *29*, 1606134.
- [17] Q.-L. Zhu, Q. Xu, *Chem. Soc. Rev.* **2014**, *43*, 5468–5512.
- [18] Y. Cui, T. Song, J. Yu, Y. Yang, Z. Wang, G. Qian, *Adv. Funct. Mater.* **2015**, *25*, 4796–4802.
- [19] Z. Wei, Z.-Y. Gu, R. K. Arvapally, Y.-P. Chen, R. N. McDougald, Jr., J. F. Ivy, A. A. Yakovenko, D. Feng, M. A. Omary, H.-C. Zhou, *J. Am. Chem. Soc.* **2014**, *136*, 8269–8276.
- [20] H. Furukawa, K. E. Cordova, M. O’Keeffe, O. M. Yaghi, *Science* **2013**, *341*, 1230444.
- [21] J. H. Cavka, S. Jakobsen, U. Olsbye, N. Guillou, C. Lamberti, S. Bordiga, K. P. Lillerud, *J. Am. Chem. Soc.* **2008**, *130*, 13850–13851.
- [22] S. Mukherjee, A. M. Kansara, D. Saha, R. Gonnade, D. Mullangi, B. Manna, A. V. Desai, S. H. Thorat, P. S. Singh, A. Mukherjee, S. K. Ghosh, *Chem. Eur. J.* **2016**, *22*, 10937–10943.
- [23] C. Yang, U. Kaipa, Q. Z. Mather, X. Wang, V. Nesterov, A. F. Venero, M. A. Omary, *J. Am. Chem. Soc.* **2011**, *133*, 18094–18097.
- [24] S. Roy, V. M. Suresh, T. K. Maji, *Chem. Sci.* **2016**, *7*, 2251–2256.
- [25] C. A. Fernandez, S. K. Nune, H. V. Annapureddy, L. X. Dang, B. P. McGrail, F. Zheng, E. Polikarpov, D. L. King, C. Freeman, K. P. Brooks, *Dalton Trans.* **2015**, *44*, 13490–13497.
- [26] C. Liu, Q. Liu, A. Huang, *Chem. Commun.* **2016**, *52*, 3400–3402.
- [27] G. Huang, Q. Yang, Q. Xu, S.-H. Yu, H.-L. Jiang, *Angew. Chem. Int. Ed.* **2016**, *55*, 7379–7383; *Angew. Chem.* **2016**, *128*, 7505–7509.
- [28] Y. Isaka, Y. Kawase, Y. Kuwahara, K. Mori, H. Yamashita, *Angew. Chem. Int. Ed.* **2019**, *58*, 5402–5406; *Angew. Chem.* **2019**, *131*, 5456–5460.
- [29] K. P. Rao, M. Higuchi, K. Sumida, S. Furukawa, J. Duan, S. Kitagawa, *Angew. Chem. Int. Ed.* **2014**, *53*, 8225–8230; *Angew. Chem.* **2014**, *126*, 8364–8369.
- [30] W. Zhang, Y. Hu, J. Ge, H.-L. Jiang, S.-H. Yu, *J. Am. Chem. Soc.* **2014**, *136*, 16978–16981.
- [31] Y. Sun, Q. Sun, H. Huang, B. Aguila, Z. Niu, J. A. Perman, S. Ma, *J. Mater. Chem. A* **2017**, *5*, 18770–18776.
- [32] K. Wenderich, G. Mul, *Chem. Rev.* **2016**, *116*, 14587–14619.
- [33] Q. Yang, Q. Xu, H.-L. Jiang, *Chem. Soc. Rev.* **2017**, *46*, 4774–4808.
- [34] J. Bi, J. Chen, Y. Dong, W. Guo, D. Zhu, T. Li, *J. Polym. Sci. Part A* **2018**, *56*, 2344–2353.
- [35] F. Zhang, M. Chen, X. Wu, W. Wang, H. Li, *J. Mater. Chem. A* **2014**, *2*, 484–491.
- [36] S. Gao, N. Zhao, M. Shu, S. Che, *Appl. Catal. A* **2010**, *388*, 196–201.
- [37] P. Rani, R. Srivastava, *Tetrahedron Lett.* **2014**, *55*, 5256–5260.
- [38] M. Annapurna, T. Parsharamulu, P. V. Reddy, M. Suresh, P. R. Likhar, M. L. Kantam, *Appl. Organomet. Chem.* **2015**, *29*, 234–239.
- [39] C. I. Ezugwu, B. Mousavi, M. A. Asrafa, A. Mehta, H. Vardhan, F. Verpoort, *Catal. Sci. Technol.* **2016**, *6*, 2050–2054.
- [40] W. Sun, L. Gao, X. Sun, G. Zheng, *Dalton Trans.* **2018**, *47*, 5538–5541.
- [41] A. K. Kar, R. Srivastava, *Inorg. Chem. Front.* **2019**, *6*, 576–589.
- [42] R. S. B. Gonçalves, A. B. V. de Oliveira, H. C. Sindra, B. S. Archanjo, M. E. Mendoza, L. S. A. Carneiro, C. D. Buarque, P. M. Esteves, *ChemCatChem* **2016**, *8*, 743–750.
- [43] X. Ren, S. Kong, Q. Shu, M. Shu, *Chin. J. Chem.* **2016**, *34*, 373–380.
- [44] V. Sadhasivam, M. Mariyappan, A. Siva, *ChemistrySelect* **2018**, *3*, 13442–13455.
- [45] A. S. Roy, J. Mondal, B. Banerjee, P. Mondal, A. Bhaumik, S. M. Islam, *Appl. Catal. A* **2014**, *469*, 320–327.
- [46] S. Pradhan, S. Dutta, R. P. John, *New J. Chem.* **2016**, *40*, 7140–7147.
- [47] J. Huang, W. Wang, H. Li, *ACS Catal.* **2013**, *3*, 1526–1536.
- [48] M. Zhang, X. Xin, Z. Xiao, R. Wang, L. Zhang, D. Sun, *J. Mater. Chem. A* **2017**, *5*, 1168–1175.

Manuscript received: August 5, 2019

Accepted manuscript online: September 10, 2019

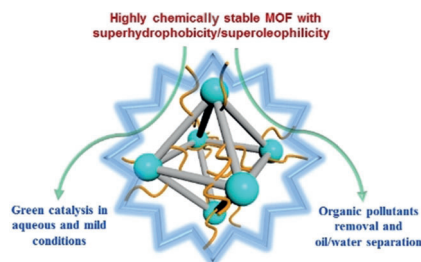
Version of record online: ■ ■ ■ ■ ■ ■ ■ ■ ■ ■

Research Articles

Green Catalysis

N.-X. Zhu, Z.-W. Wei, C.-X. Chen,
D.-W. Wang, C.-C. Cao, Q.-F. Qiu,
J.-J. Jiang, H.-P. Wang,
C.-Y. Su* ————— ■■■■-■■■■

Self-Generation of Surface Roughness by
Low-Surface-Energy Alkyl Chains for
Highly Stable Superhydrophobic/
Superoleophilic MOFs with Multiple
Functionalities



Simply super: Alkyl chains were introduced into the organic linkers of UiO-67 to provide highly chemically stable hydrophobic MOFs. The alkyl groups protected the hydrophilic Zr_6O_8 clusters and made the MOF interspace superoleophilic, as well as generating a rough crystal surface for superhydrophobicity. The MOFs are suitable for oil/water separation and water purification, and were modified with metal-binding ligands for environmentally friendly catalysis.